Stochastic Semi-Implicit Substep Method for Coupled Depletion Monte-Carlo Codes

D. Kotlyar and E. Shwageraus

Department of Engineering, University of Cambridge
CB2 1PZ, Cambridge, United Kingdom

Keywords:
Monte Carlo; depletion; coupling; BGCore; implicit; substep;

Abstract

Coupled Monte Carlo burnup codes aim to evaluate the time evolution of different parameters, such as nuclide densities, for accurate modeling of the different reactor designs and associated fuel cycles. Recently a major deficiency in numerical stability of existing Monte Carlo coupling schemes was identified. Alternative, stable coupling schemes were derived, implemented and verified. These methods are iterative and rely on either the end- or middle-of-step (MOS) reaction rates to evaluate the end-of-step (EOS) nuclide densities. Here, we demonstrate that applying the EOS methods for realistic problems may lead to highly inaccurate results. Considerable improvement can be made by adopting MOS method but the accuracy may still be insufficient. The solution proposed in this work relies on the substep method that allows reducing the time discretization errors. The proposed and tested substep method also assumes that the reaction rates are linear functions of the logarithm of the nuclide densities. The method was implemented in BGCore code and subsequently used to perform a series of test case calculations. The results demonstrate that better accuracy and hence efficiency can be achieved with negligible additional computational burden.

1. Introduction

Monte Carlo (MC) neutron transport codes are increasingly widely used as a standard calculation tool in reactor analysis. In order to evaluate fuel isotopic changes as a function of time, MC transport code must be linked to a deterministic point depletion solver. Up to day, many MC-burnup coupling programs have been developed and shown to produce accurate results, for example as shown in Bomboni et al., 2010. Among such coupled codes are SERPENT (Leppänen et al., 2015), BGCore (Fridman et al., 2008), MCNPX (Fensin et al., 2010) and many others. There is currently an on-going trend to use these codes for full core analysis (Damian and Brun, 2015).

One of the important aspects, which differ among the various codes, is the coupling scheme used to integrate MC with burnup calculations. In recent studies, a major deficiency of the current coupling schemes was reported by Dufek and Hoogenboom, (2009), Dufek et al., (2013a), and Kotlyar and Shwageraus, (2013). Their research has shown that applying existing explicit methods for coupled MC calculations may result in oscillatory behavior of local and integral parameters. This stimulated the need to adopt new, numerically stable, methods to be used in MC coupled codes. In response to this need, new coupling methods have been developed first for MC-burnup applications (Dufek et al., 2013b) and eventually followed by the more comprehensive fully coupled MC-burnup-thermal hydraulic (TH) schemes (Kotlyar and Shwageraus, 2014). The methods were implemented in the BGCore code and were shown to produce numerically stable results. The numerical stability issues were resolved through the use of alternative methods denoted as the SIE and SIMP. The methods solve the depletion and TH problems simultaneously and iteratively. Each iteration updates either the end-of-step (SIE) or middle-of-step (SIMP) flux, which is weighted with variable under-relaxation factor and combined with the values obtained in previous iterations. These methods were shown to solve the stability issue. The comparison of the various methods (i.e. SIE, SIMP and explicit) in terms of accuracy is reported here.

The SIE method, as will be shown later, may be inaccurate since it relies on the end-of-step (EOS) parameters, such as reaction rates, to calculate the EOS nuclide densities. In realistic problems, with rapid change of spectrum for example, this EOS

approach could lead to a systematic under (or over) prediction of some reaction rates. However, even more alarming is the fact that the iterative approach required to stabilize the solution may deteriorate its accuracy even further. More specifically, as the number of iterations increases, the under or over prediction becomes greater. The SIMP method that relies on the middle-of-step quantities is much more accurate than SIE. However, the method also relies on the constant reaction rates (MOS) throughout the analyzed timestep, which is only an approximation to reality. It appears that these errors are a result of not knowing the precise shape of the reaction rates versus time function within the time interval.

Therefore, this work focuses on extending the stochastic implicit Euler methodology with the substep method and will be denoted here as the SUBSTEP. The method uses a log-linear correlation between the nuclide densities and reaction rates to better account for the variation in reaction rates within the timestep. The method requires only additional depletion calculations to be carried out with no additional transport calculations and therefore has negligible computational burden.

The method was implemented in BGCore code, which was subsequently used to perform three, 2 and 3-dimensional (2D and 3D), test calculations of typical PWR fuel pin and assembly models. The results systematically show that the proposed method outperforms the original SIE and SIMP methods in accuracy and therefore computational efficiency.

2. BGCore description

The proposed SUBSTEP method was programmed into BGCore system. BGCore is a system of codes developed at Ben-Gurion University, in which Monte-Carlo code MCNP4C is coupled with fuel depletion and decay module. BGCore utilizes multi-group methodology for calculation of one-group transmutation cross-sections (Haeck et al., 2007; Fridman et al., 2008) which significantly improves the speed of burnup calculations. In addition to the depletion module, BGCore system also includes a built-in thermal-hydraulic (TH) feedbacks module. The modules are executed iteratively so that the coupled system is capable of predicting fuel composition, power, coolant density and temperature distributions in various types of reactor systems (Kotlyar et al., 2011).

3. Burnup coupling methodology

The depletion equations use time dependent fluxes, although still assumed to be constant for each time step, to determine the evolution of nuclide inventories with time. However, nuclide inventories depend on the flux, which by itself requires a prior knowledge of the nuclide inventories. There are several approaches to solve this non-linear problem.

First, the solution requires discretizing the full time scale into time steps, in which the parameters of interest (i.e. reaction rates and nuclide densities) are to be computed. At each time step, the procedure requires solving 2 independent problems. The first is the neutron transport eigenvalue equation that provides reaction rates. In this work, it will be denoted by the operator $\varphi(\mathbf{N})$. MCNP4C code is used here to obtain the reaction rates $\mathbf{X} = \varphi(\mathbf{N})$ for a known mixture of $\mathbf{N}$ different nuclides.

In order to progress in time, the Bateman equations (Bateman, 1932) which have the matrix exponential solution (Eq. 1) must also be solved.

$$\mathbf{N}(t) = e^{\boldsymbol{\mathcal{M}}\Delta t}\mathbf{N}(0) \tag{1}$$

where, $\mathbf{N} = [n_1 \cdots n_n]$ is unique for a certain time point and n_j is the atomic nuclide density of nuclide j. BGCore follows the evolution of *n=1743* nuclides for accurate estimation of decay heat and radiotoxicity following shutdown. The operator $\boldsymbol{\mathcal{M}}$ in Eq.1 represents the transmutation matrix which depends on the reaction rates $\mathbf{X}$. The relation between $\boldsymbol{\mathcal{M}}$ and $\mathbf{X}$ is described in Eq.2:

$$\boldsymbol{\mathcal{M}}(t) = \boldsymbol{\Lambda} + \mathbf{X}(t) \tag{2}$$

where, $\boldsymbol{\Lambda}$ is the decay matrix and includes removal terms on its diagonal and production rates on the off-diagonal as explained in Eq.3:

$$\begin{aligned} \Lambda_{j,j} &= -\lambda_j \\ \Lambda_{j,k\neq j} &= \lambda_{k\rightarrow j} \end{aligned} \tag{3}$$

where λ_j is the decay constant of nuclide j and $\lambda_{k\rightarrow j}$ is the decay constant from nuclide k to nuclide j. This matrix is pre-generated and remains constant through the entire fuel cycle calculations.

$\mathbf{X}$ is the neutron induced transmutation matrix that is obtained from the transport solution for a pre-determent $\mathbf{N}$ and therefore is unique at each time point. The diagonal elements of this matrix are removal rates following neutron absorption and

the off-diagonal elements describe the production from other reactions (e.g. fission, inelastic scattering, etc.) as described in Eq.4:

$$\begin{aligned} \mathrm{X}_{j,j} &= -\sigma_j \phi \\ \mathrm{X}_{j,k\neq j} &= \sigma_{k\rightarrow j} \phi \end{aligned} \tag{4}$$

Where, σ_j is the energy average absorption cross section of nuclide *j*, $\sigma_{k\rightarrow j}$ is the average cross section of nuclide *k* which leads to *j* and ϕ is the 1-group flux.

As mentioned earlier, in fuel cycle calculations, the irradiation time is divided into time steps. At each timestep, the transport and depletion problems are solved independently (operator splitting approach) and the solutions are iteratively coupled in a designated subroutine. The coupling scheme determines the accuracy and numerical stability of the solution.

Section 3.1 describes the explicit Euler method implemented in many of the existing computational tools used in reactor physics analyses. This is then followed by the SIE and SIMP algorithms introduction in Sections 3.2 and 3.3 respectively. Lastly, the newly proposed SUBSTEP algorithm is presented in Section 3.4. The different numerical schemes in these sections describe the coupling procedure to solve a single timestep depletion $\forall t \in [t_0, t_1]$ with timestep length $\Delta t = t_1 - t_0$. In addition, $\mathbf{N}_i$ and $\boldsymbol{\mathcal{M}}_i$ are the nuclide density vector and transmutation matrix at t_i respectively.

3.1 Explicit Euler method

According to the explicit Euler method, the neutron transport solution is obtained at the beginning-of-step (BOS) for a pre-determined fuel inventory. Then, the space and energy dependent microscopic reaction rates are assumed to be constant during the depleted time step. Knowing these reaction rates allows obtaining the concentration at the end-of-step (EOS) in a single calculation step.

1 $\boldsymbol{\mathcal{M}}_0 \longleftarrow \varphi(\mathbf{N}_0)$
2 $\mathbf{N}_1 \longleftarrow e^{\boldsymbol{\mathcal{M}}_0 \Delta t} \mathbf{N}_0$

3.2 Stochastic implicit Euler (SIE) method

SIE (Dufek et al., 2013b) is a recently proposed method that uses EOS values of reaction rates to calculate EOS quantities of interest (i.e. nuclide densities). The solution is obtained by using the so-called stochastic approximation with under-relaxation factor based on the Robbins-Monro algorithm (Robbins and Monro, 1951). The relaxation algorithm could be either applied to the nuclide density field (i.e. SIE/ND) or the flux field (i.e. SIE/FLUX). The mathematical derivation of the methods and their implementation is presented in the original paper and hence will not be repeated here.

Since the coupled MC calculations are computationally expensive, only the performance of the SIE/ND method is evaluated here. However, the results for the SIE/FLUX method are expected to be similar and the conclusions would be identical. The SIE/ND algorithm presented here and through-out this paper will be referred as SIE.

In the proposed SIE method, the depletion calculations are performed with end-of-step flux and cross sections ($\boldsymbol{\mathcal{M}}_1$) rather than BOS quantities.

1 $\boldsymbol{\mathcal{M}}_0 \longleftarrow \varphi(\mathbf{N}_0)$

2 $\bar{\mathbf{N}}_1 = \mathbf{N}_1^{(0)} \longleftarrow e^{\boldsymbol{\mathcal{M}}_0 \Delta t}\mathbf{N}_0$

3 ***for*** $\kappa = 1 : \kappa_{max}$

4 $\boldsymbol{\mathcal{M}}_1^{(\kappa)} \longleftarrow \varphi(\bar{\mathbf{N}}_1)$

5 $\mathbf{N}_1^{(\kappa)} \longleftarrow e^{\boldsymbol{\mathcal{M}}_1^{(\kappa)} \Delta t}\mathbf{N}_0$

6 $\bar{\mathbf{N}}_1 = \sum_{i=1}^{\kappa} \frac{\mathbf{N}_1^{(i)}}{\kappa}$

7 ***End for***

3.3 Stochastic implicit mid-point (SIMP) method

SIMP (Kotlyar and Shwageraus, 2014) is another recent method that uses a philosophy similar to that adopted for the SIE method. However, the convergence procedure is performed with the middle-of-step (MOS) or time step-averaged quantities rather than the EOS ones. The relaxation algorithm could be applied either to the nuclide density field (i.e. SIMP/ND) or to the flux field (i.e. SIMP/FLUX). The

mathematical derivation is presented in the original paper and hence will not be repeated here. Only the performance of the SIMP/ND (denoted as SIMP) method will be reported. However, the results for the SIMP/FLUX method are expected to be similar.

In the proposed SIMP method, the depletion calculations are performed with middle-of-step (i.e. at $t_{0.5} = \frac{t_1+t_0}{2}$) flux and cross sections ($\boldsymbol{\mathcal{M}}_{0.5}$).

1 $\boldsymbol{\mathcal{M}}_0 \leftarrow \varphi(\mathbf{N}_0)$

2 $\bar{\mathbf{N}}_1 = \mathbf{N}_1^{(0)} \leftarrow e^{\boldsymbol{\mathcal{M}}_0 \Delta t}\mathbf{N}_0$

3 ***for*** $\kappa = 1{:}\,\kappa_{max}$

4 $\boldsymbol{\mathcal{M}}_{\mathbf{0.5}}^{(\kappa)} \leftarrow \varphi\left(\bar{\mathbf{N}}_{0.5} = \frac{\bar{\mathbf{N}}_1 + \mathbf{N}_0}{2}\right)$

5 $\mathbf{N}_1^{(\kappa)} \leftarrow e^{\boldsymbol{\mathcal{M}}_{0.5}^{(\kappa)} \Delta t}\mathbf{N}_0$

6 $\bar{\mathbf{N}}_1 = \sum_{i=1}^{\kappa} \frac{\mathbf{N}_1^{(i)}}{\kappa}$

7 ***End for***

3.4 Stochastic Semi-Implicit Substep (SIE) method

The methods presented in Sections 3.1, 3.2 and 3.3 are limited to a constant power/flux approximation, in which either the BOS, EOS or MOS reaction rates are considered to be representative of the entire timestep. The stochastic semi-implicit substep (denoted as SUBSTEP) method presented here was inspired by the two main recently presented methods:

1. The Substep scheme for coupled MC codes was originally introduced by (Isotalo and Aarnio, 2011a). The method relied on dividing the depletion step into substeps and solving the depletion problem separately for each substep. In order to do so, a relation between reaction rates and time must be established. The authors showed that this method considerably improves the accuracy of the coupled MC codes. It must be noted however, that the reaction rates dependence on time may somewhat deviate from the real one. For the sake of the discussion, let us assume that the following procedure is used to obtain the time dependent reaction rates. The procedure starts by obtaining the reaction rates at t_0 which are then used in the depletion routine to predict the EOS nuclide densities at t_1. Thereafter, a corrector step is carried out, for which the predicted reaction rates are used to re-calculate the EOS nuclide densities. The drawback of such scheme is that the predicted reaction rates at t_1 were obtained by using the t_0 reaction rates, which are not real time-point (i.e. at t_1) representative.
2. An improved log linear rate (LLT) method (Carpenter et al., 2010) has been developed and tested in MC21 Monte Carlo code (Sutton et al., 2007). This method assumes the reaction rates are linear functions of the natural logarithm of the nuclide densities. In the mentioned work, this approximation was applied to Gd nuclides. The paper also implied that this correlation may only be used only for nuclides with strong self-shielding. The method is an extension of the projected predictor-corrector (PPC) method, suggested by Yamamoto et al. (2008) that assumes linear relation between the reaction rates and atom densities. The PPC method, however, was shown to produce less accurate results than the LLT when the timestep size was increased.

These methods were incorporated into the SIE iterative scheme to produce more accurate results. The main idea is to create a relation between the reaction rates and the logarithm of nuclide densities (stage 5) and then apply the substep method (stages 7 through 10) to account for the reaction rates change as a function of nuclide densities (stage 8), which are also a function of time (stage 9).

1 $\boldsymbol{\mathcal{M}}_0 \longleftarrow \varphi(\mathbf{N}_0)$

2 $\bar{\mathbf{N}}_1 = \mathbf{N}_1^{(0)} \longleftarrow e^{\boldsymbol{\mathcal{M}}_0 \Delta t}\mathbf{N}_0$

3 $\boldsymbol{for}\ \kappa = 1{:}\,\kappa_{max}$

4 $\boldsymbol{\mathcal{M}}_1^{(\kappa)} \longleftarrow \varphi(\bar{\mathbf{N}}_1)$

5 $$\boldsymbol{\mathcal{M}}_t = \frac{\boldsymbol{\mathcal{M}}_1^{(\kappa)} - \boldsymbol{\mathcal{M}}_0}{\log_e \frac{\bar{\mathbf{N}}_1}{\mathbf{N}_0}} \log_e \frac{\mathbf{N}_t}{\mathbf{N}_0} + \boldsymbol{\mathcal{M}}_0$$

6 $\mathbf{N}_\ell^{(\kappa)} = \mathbf{N}_0$

7 $\boldsymbol{for}\ \ell = 1{:}\,\ell_{max}$

8 $$\boldsymbol{\mathcal{M}}_\ell = \frac{\boldsymbol{\mathcal{M}}_1^{(\kappa)} - \boldsymbol{\mathcal{M}}_0}{\log_e \frac{\bar{\mathbf{N}}_1}{\mathbf{N}_0}} \log_e \frac{\mathbf{N}_\ell^{(\kappa)}}{\mathbf{N}_0} + \boldsymbol{\mathcal{M}}_0$$

9 $$\mathbf{N}_\ell^{(\kappa)} \longleftarrow e^{\boldsymbol{\mathcal{M}}_\ell \times \frac{\Delta t}{\ell_{max}}}\mathbf{N}_{\ell-1}^{(\kappa)}$$

10 $\boldsymbol{End\ for}{:}\ \ell$

11 $$\bar{\mathbf{N}}_1 = \sum_{i=1}^{\kappa} \frac{\mathbf{N}_1^{(i)}}{\kappa}$$

12 $\boldsymbol{End\ for}{:}\ \kappa$

The variables $\mathbf{N}_t$ and $\boldsymbol{\mathcal{M}}_t$ in stage 5 are nuclide densities and reaction rates vectors as a function of time, respectively. These vectors are constructed from knowing the BOS $\mathbf{N}_0$ and $\boldsymbol{\mathcal{M}}_0$ and EOS $\mathbf{N}_1$ and $\boldsymbol{\mathcal{M}}_1$ values. It should also be mentioned that stages 5 and 8 are performed in a matrix-wise operation. In the current study, this linear-log correlation was adopted for all nuclides and reaction rates. At zero burnup, where most nuclides are present at zero concentration, a very small

values of 10^{-30} was assigned to all the nuclides to avoid machine precision errors (i.e. $\log_e 0$).

The method presented here is a general one and can be used in problems where numerical oscillations may appear. However, in order to avoid additional computational burden, the method can be greatly simplified by setting κ_{max} to unity, i.e. performing a single EOS iteration.

Moreover, since the method relies on iterations to stabilize the solution, more data points are produced during iterations (i.e. $\boldsymbol{\mathcal{M}}_i$ **vs.** $\mathbf{N}_i$) and these could be used to establish better fit than using only 2 points. The use of higher order methods (Isotalo and Aarnio, 2011b) to link the $\mathbf{N}_t$ and $\boldsymbol{\mathcal{M}}_t$ may also lead to a better overall accuracy. However, these options have not been investigated in the current research.

4. Results and discussion

In previous studies (Dufek et al., 2013a, Kotlyar and Shwageraus, 2013), typical PWR 3D fuel pin and assembly cases were chosen to demonstrate the potentially unstable behavior of the explicit method. In order to address this issue, the SIE and SIMP methods were introduced and shown to be effective in eliminating the problems observed when using explicit methods.

Here, we show that in cases where the flux amplitude and spectrum change rapidly with time, the accuracy of the SIE method is questionable. The results produced by the mid-point SIMP method are much more accurate but could be further improved. To reduce the computational costs, only the results of SIE/ND (Dufek et al., 2013a) and SIMP/ND (Kotlyar and Shwageraus, 2014) methods are presented.

The accuracy issues of the methods developed previously and the verification of the proposed, SUBSTEP, method was performed by examining 3 cases, as described in sections 4.1 through 4.3.

4.1 PWR 2D mini-assembly

A 9x9 array of PWR pins with UO_2 fuel and water cooled is examined in this section. The initial fuel enrichment was taken to be 3.5 w/o. The fuel in the central pin was also mixed with 1.5 v/o of Gd_2O_3. The central pin was subdivided into 5 equal-volume regions to realistically track the spatial burnup of Gd isotopes and its effect on the system's criticality. Schematic view and operating parameters of the considered UO_2 test case are given in Fig. 1 and Table 1.

In order to assure the fission source convergence and obtain relatively small statistical uncertainties, 200 active fission source iteration cycles with 100,000 histories per cycle were used in the neutron transport calculations with MCNP.

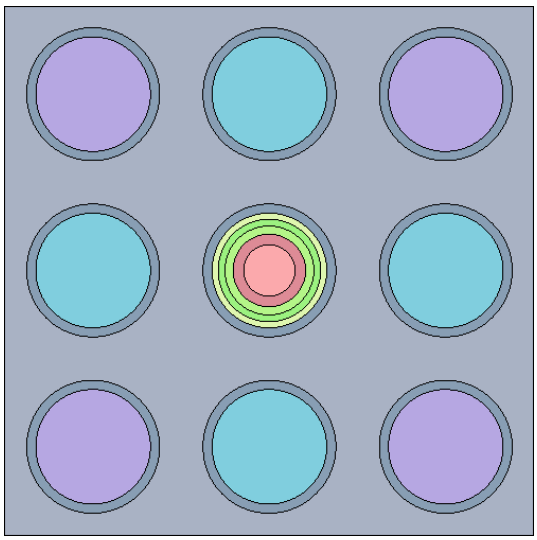

Fig. 1. PWR mini-assembly geometry

Table 1: Summary of the mini-assembly design parameters

Parameter	**Value**
Fuel pellet diameter, cm	0.8100
Fuel pin diameter, cm	0.9500
Fuel-cladding thickness, cm	0.0655
Fuel lattice pitch, cm	1.2600
Number of pins per assembly	9
Fuel / clad and coolant temperature, K	900/600
Power, W/cm^3	104

The chosen problem includes Gd absorber that strongly affects the system's spectrum and hence its criticality as shown in Fig. 2. It can be seen that as the Gd poison depletes, the criticality increases and reaches a peak at around 160 days. In the current study, only the time interval between 0 and 210 days was analyzed to illustrate the accuracy of the previously proposed SIE and SIMP schemes.

The reference solution was obtained by using explicit Euler method with very fine timesteps of 0.25 days or 0.009 MWd/kg. The convergence of the reference solution was verified by decreasing the timesteps' length from values of 2 days down to 0.25 days. When the timestep was varied from 0.5 days to 0.25, the differences in the results were within the statistical uncertainties. The solutions with the explicit, SIE, SIMP and SUBSTEP methods were first obtained for time steps of 5 days and then repeated for more practical steps of 20 days.

Since SIE, SIMP and SUBSTEP methods use iterative scheme, the results were obtained for an arbitrary chosen number of iterations, in this case 10.

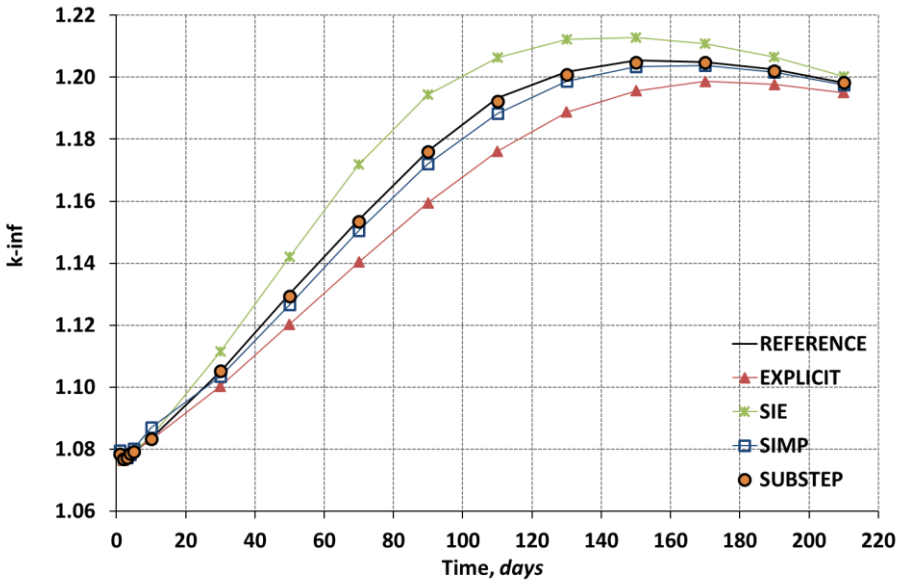

Fig. 2. k-inf as a function of time, mini-assembly case

Fig. 3 depicts the relative difference (%) between the reference and the four studied coupling schemes in concentration of Gd^{157}, which has a high absorption rate, as a function of time. Fig. 3a shows that the explicit method considerably over-predicts the concentration of Gd^{157}, whereas SIE significantly under-predicts the concertation. This over- and under-prediction of Gd^{157} density leads in turn to under- and over-prediction of k-inf as shown in Fig. 4a. Statistical uncertainties as a function of burnup are also reported in this figure. These values correspond to 1 standard deviation values (~50 pcms) obtained directly from MCNP. The accuracy of the results deteriorates further when the time step is increased from 5 days to 20 days (Fig. 3b and Fig. 4b). The results produced by SIMP are much more accurate, with a Gd^{157} peak difference of 2.5% and 9.7% when 5 days and 20 days timesteps are used respectively. These figures clearly show that the proposed SUBSTEP method outperforms all previously developed methods. The Gd^{157} peak difference is below 0.1% and 1% when 5 days and 20 days timesteps are utilized.

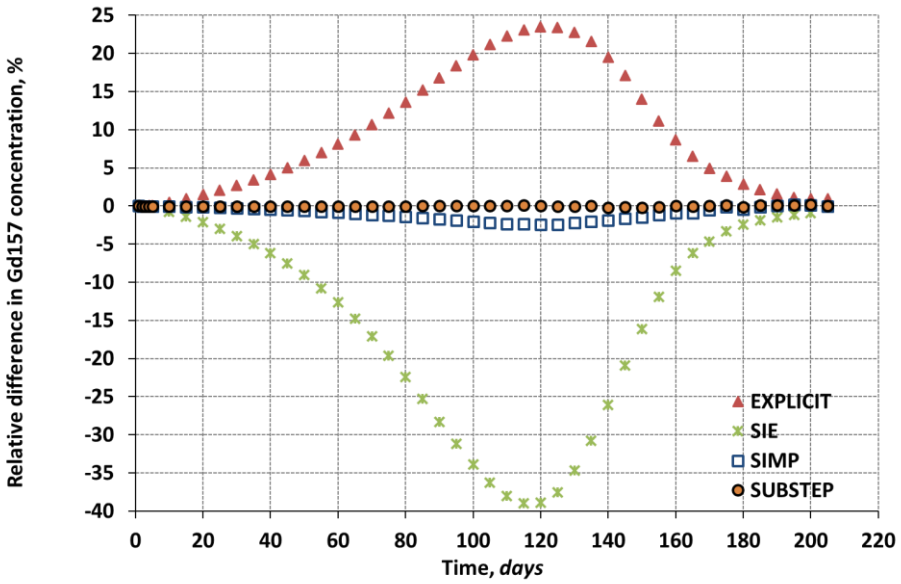

(a) 5 days

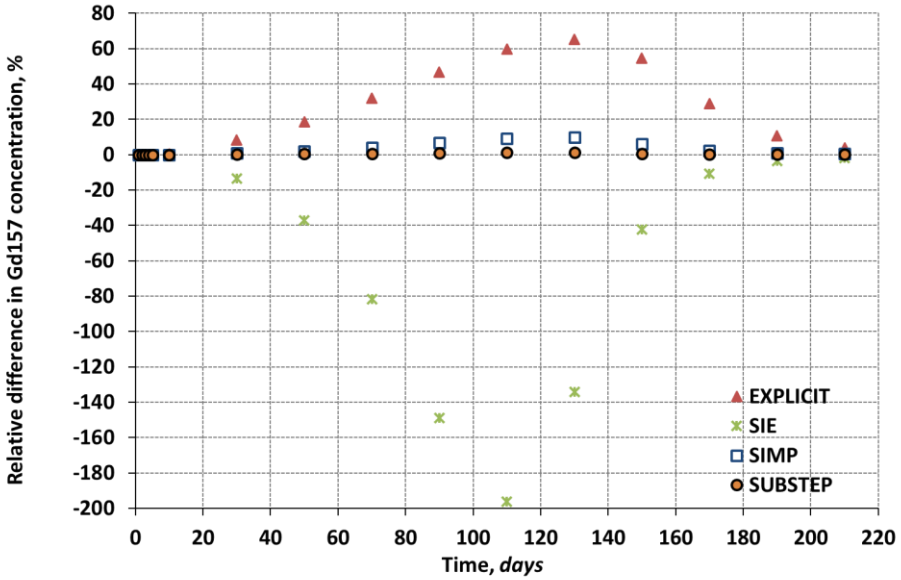

(b) 20 days

Fig. 3. Comparison of Gd^{157} concentration for various coupling schemes, mini-assembly case

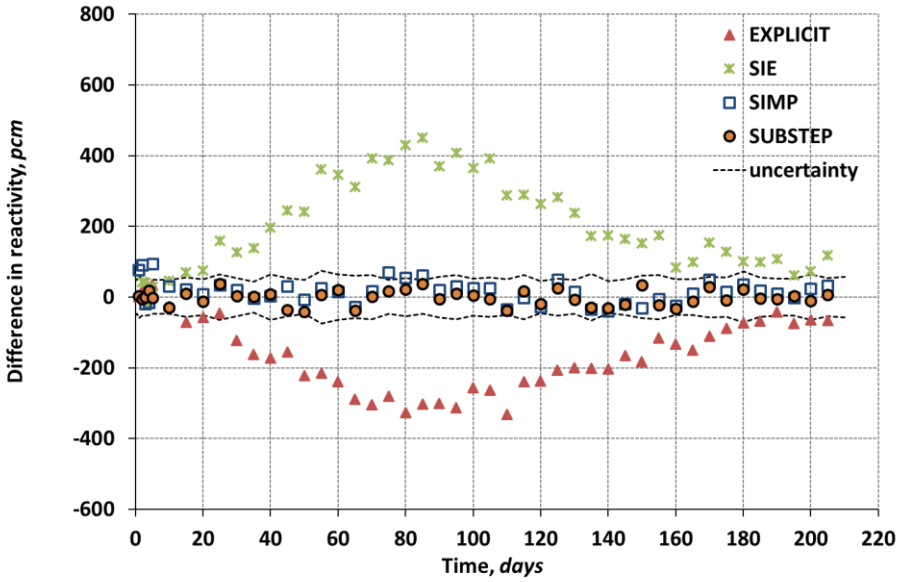

(a) 5 days

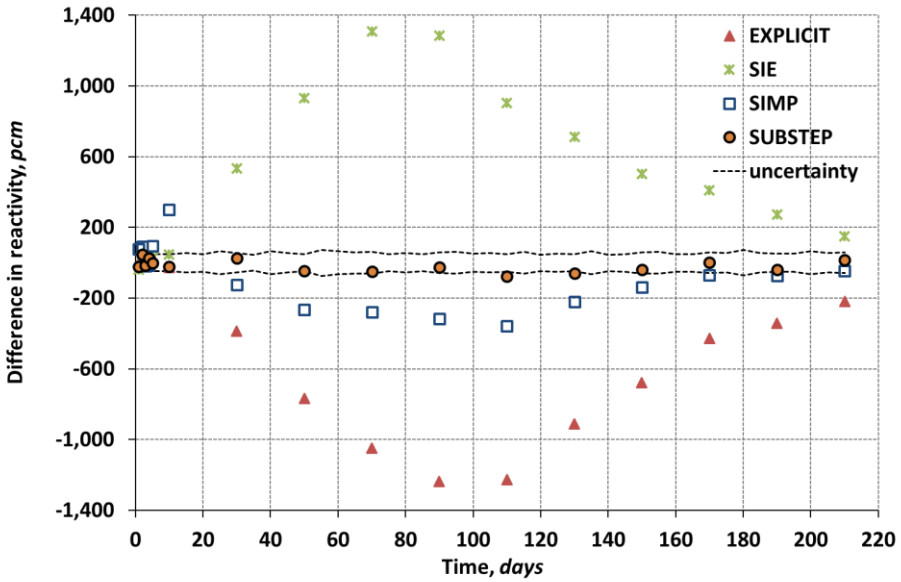

(b) 20 days

Fig. 4. Comparison of k-inf for various coupling schemes, mini-assembly case

Fig. 5 shows rather remarkable result. Contrary to the expectation, increasing the number of iterations in the SIE method actually reduces the accuracy in a systematic manner rather than improves it. For example, the maximum difference in Gd^{157} concentration monotonically grows from -50% up to -196% when the number of iterations in increased from 3 to 10.

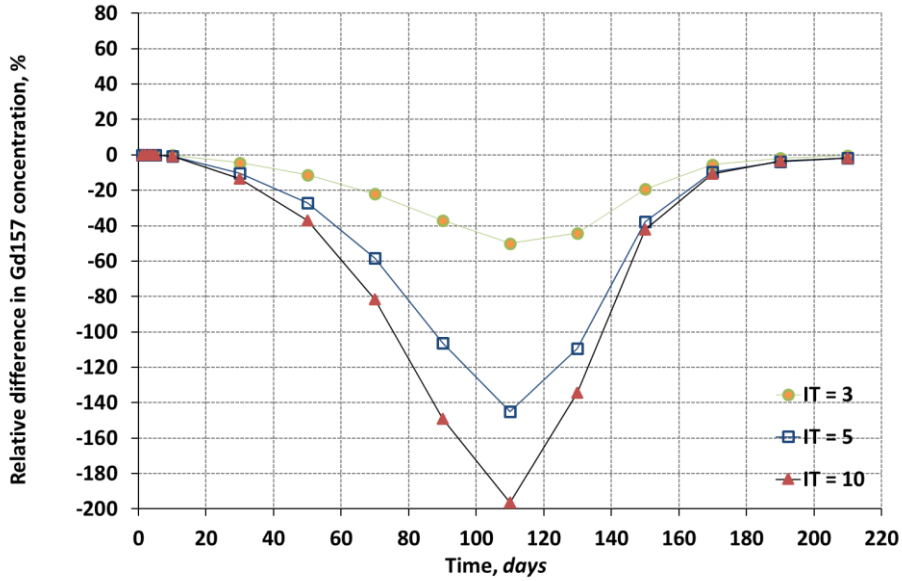

Fig. 5. Comparison of Gd^{157} concentration for SIE method (timestep of 20 days), mini-assembly case

Fig. 6 explains the surprising behavior of the SIE method. For illustration purposes, a time interval of 20 days was examined. At the BOS, the inventories of all the nuclides were fixed.

The reference solution was obtained by depleting the problem with 0.25 days. Then, the reference (i.e. timestep average) capture reaction rates in Gd^{157} as reported in Fig. 6 by the horizontal line was calculated according to Eq.5.

$$\overline{N\sigma_c\phi} = \frac{\int_0^{20} \sigma_c(t)\,\phi(t)dt}{\Delta t} \tag{5}$$

The SIE method (green triangles in Fig. 6) was applied first to reproduce the reference solution at 20 days in a single step. Fig. 6 shows that the EOS (at 20 days) cross section is over-predicted (by ~18%) when the SIE method is used. The explanation is fairly simple. The 1st iteration in the SIE method obtains the reaction rates (i.e. MCNP) at 0 days. Then, these reaction rates are used to deplete the problem with 20 day time step and obtain the new concentration. With no iterations, the scheme would be identical to the explicit Euler method and would result in over-estimation of the real end of time step Gd concentration since the BOS reaction rates (smaller than time step-average Gd cross section) were used for the entire step. The transport solution at the EOS is obtained with the new nuclide densities and produce new reaction rates. Since, the Gd^{157} depletes rapidly, the spectrum "softens" quickly and the EOS cross section is increased. Therefore, with each new iteration, we artificially increase the value of the Gd^{157} cross section and impose this value as the whole time-interval representative. It should be noted that for the SIE case, the convergence of the Gd^{157} cross section is achieved due to the variable under-relaxation factor (1/n, where n is the iteration number) on the nuclide density field used in SIE method.

The reason that SIE performs poorly is the lack of information regarding the time-dependent reaction rates within the 20 days interval. The new extension of the SIE method, which is designated as the SUBSTEP allows to reproduce this information and therefore to achieve more accurate results (0.03% difference). SIMP under-predicts the reaction rates by ~2.5%.

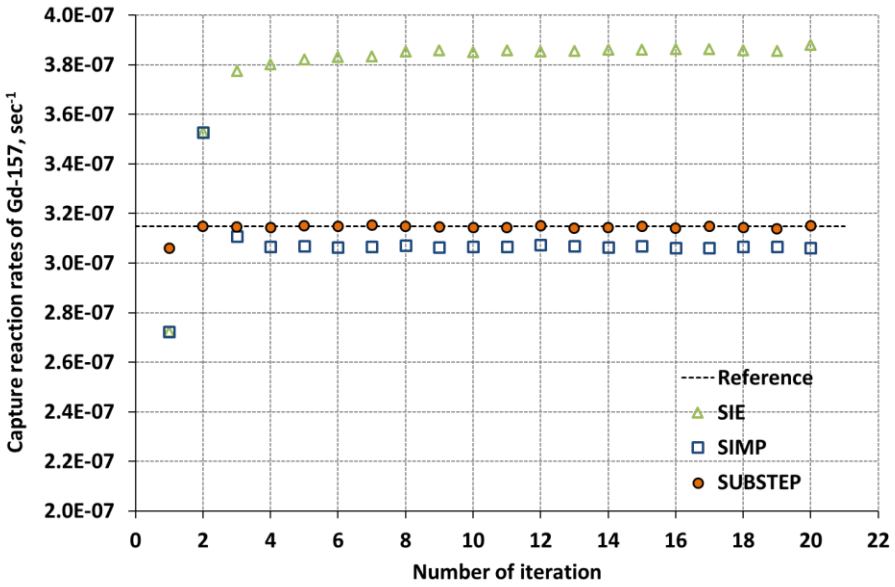

Fig. 6. Comparison of Gd157 microscopic reaction rates

Fig. 7 shows why methods that rely on constant reaction rates approximation fail to reproduce the reference solution. The figure shows that the cross section of Gd^{157} in the course of 25 days roughly doubles and therefore neither the BOS nor EOS values can be taken as the timestep-representative. Fig. 8 that presents the results for outermost ring demonstrates the effectiveness of the logarithmic–linear correlation between the nuclide densities and reaction rates. For this purpose, the parameters, i.e. the reaction rates and nuclide densities, at t=30 days and 75 days were obtained directly from the reference solution (0.25 days steps). Only these 2 points were used to plot the log/linear and linear/linear curves. In addition, Fig. 9 presents the normalized absorption reaction rates for different nuclides as a function of concentration. Two correlations were applied, i.e. Linear-Log (Fig. 9a) and Linear-Linear (Fig. 9b). Both correlations seem to fit well, however only the Linear-Log was chosen in this study as representative for all nuclides. This is because different correlations for various nuclides would somewhat complicate the procedure presented in section 3.4.

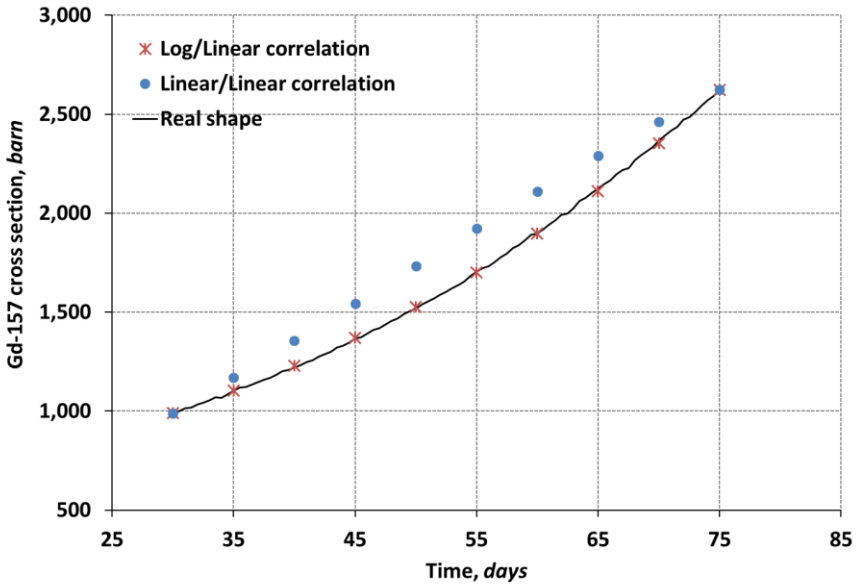

Fig. 7. Gd^{157} microscopic cross section as a function of time

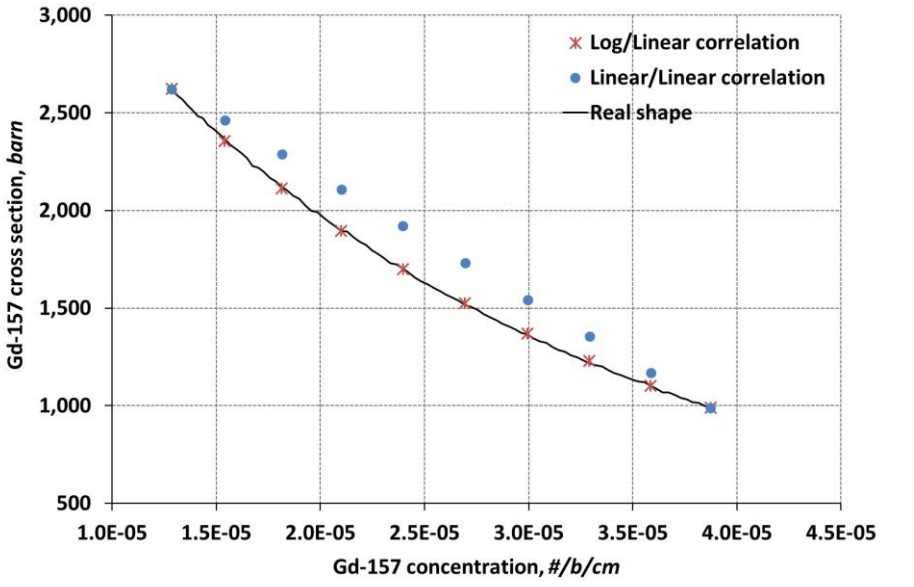

Fig. 8. Gd^{157} microscopic cross section as a function of its concentration

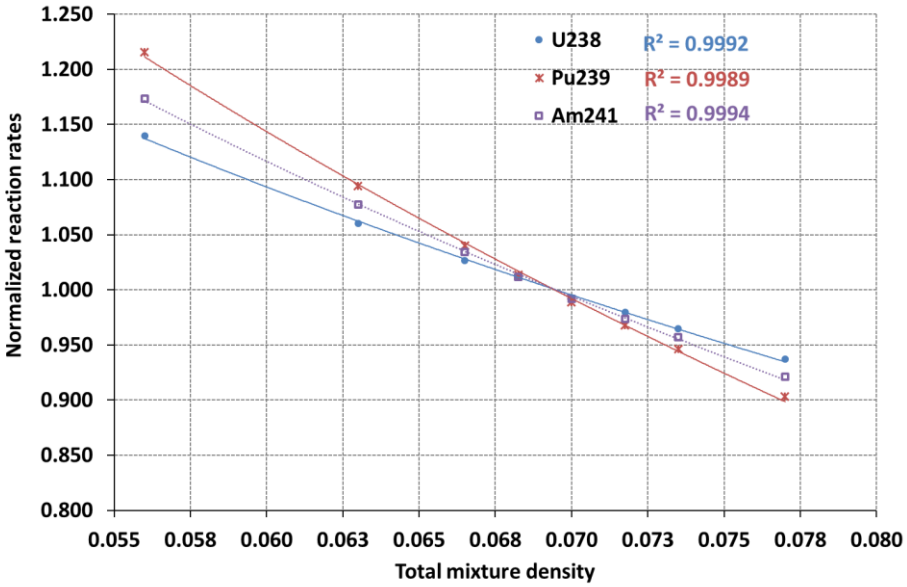

a. Linear-Log correlation

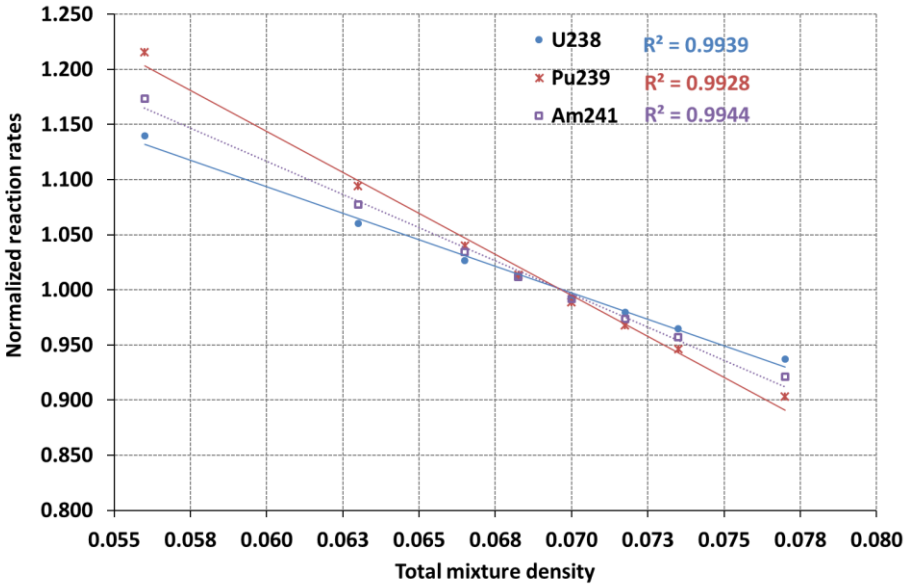

b. Linear-Linear correlation

Fig. 9. Normalized absorption reaction rates as a function of concentration

4.2 PWR 3D unit cell

A 3D fuel unit cell similar to that used in our previous analysis (Dufek et al., 2013b) was used here as an additional test case. This case is characterized by its high dominance ratio (Dumonteil and Courau, 2010) which makes it difficult for the source iterations in the MC procedure to reach convergence. As a result, there is always a slight deviation of the local flux from the real uniform shape. This in turn leads to oscillations in local parameters when explicit methods are used. Previous analyses focused on the stability characteristics of the SIE methods and indeed concluded that stability issues are resolved. Here, the aim is to show that even for this relatively simple case, where the spectrum varies slowly with time, the SIE method lacks the sufficient accuracy which is significantly improved when the SUBSTEP method is utilized.

The radial and axial schematic views of the examined case are illustrated in Fig. 10. The pin dimensions and materials are identical to the ones reported in Table 1. The 300 cm unit cell was axially halved to create two regions which include identical materials at the beginning of the irradiation campaign. The bottom and upper parts have void boundary conditions to decrease the dominance ratio and therefore reduce the number of histories required for source convergence. As a result, 5000 active fission source iteration cycles with 5,000 histories per cycle were used in neutron transport calculations with MCNP. The different coupling approaches (with 50 days timesteps) were compared to the reference solution, which was obtained with the Euler explicit method. This solution was obtained by using a single burnable material and hence a single flux value which eliminated the chance for any oscillations. Moreover, the reference solution was obtained using fine time steps of 5 days. A fixed and arbitrary number of 6 iterations was used in all methods, i.e. SIE, SIMP and SUBSTEP.

The results are presented in Fig. 11 and clearly show that the SUBSTEP method outperforms the SIE without any compromise on its stability properties. This figure shows the local flux in the bottom region as a function of time. The current results again show that explicit methods may produce highly questionable results when used for analyzing 3D problems. The results obtained with the explicit method show flux oscillations that become more severe as the timestep size is increased. While the SIE, SIMP and SUBSTEP methods produce stable results, the SIE consistently under-

predicts the 1-g flux. This happens since the spectrum is slightly softens with time and the value of the 1-g fission cross section of U^{235} is increased with time. In this test case, the SIE method tends to slightly over-predict the fissile inventory and therefore less flux is required to preserve a fixed power. It must be pointed out that the effect on criticality is less pronounced in this case. The maximum reactivity difference between the explicit, SIE, SIMP and SUBSTEP methods and the reference solution were 200, 41, 27 and 20 pcm respectively. Where the statistical uncertainty obtained directly from the MC transport solution was on the order of 18 pcm.

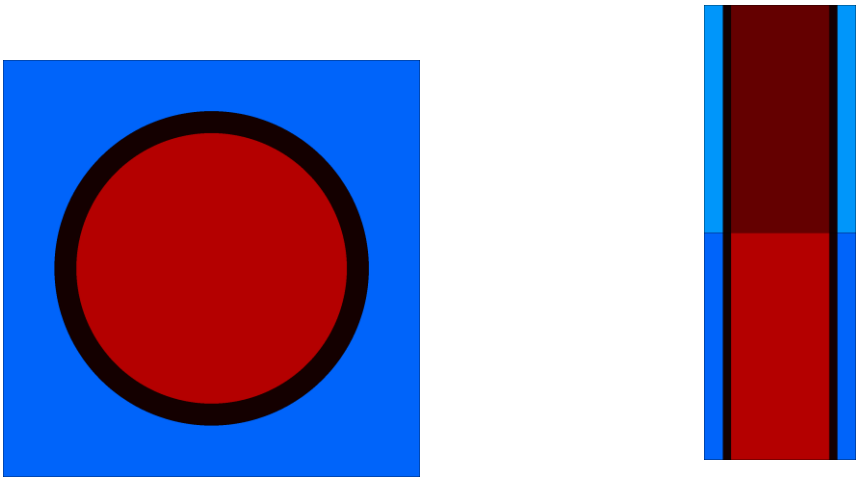

(a) x-y view (b) x-z view

Fig. 10. PWR 3D unit cell

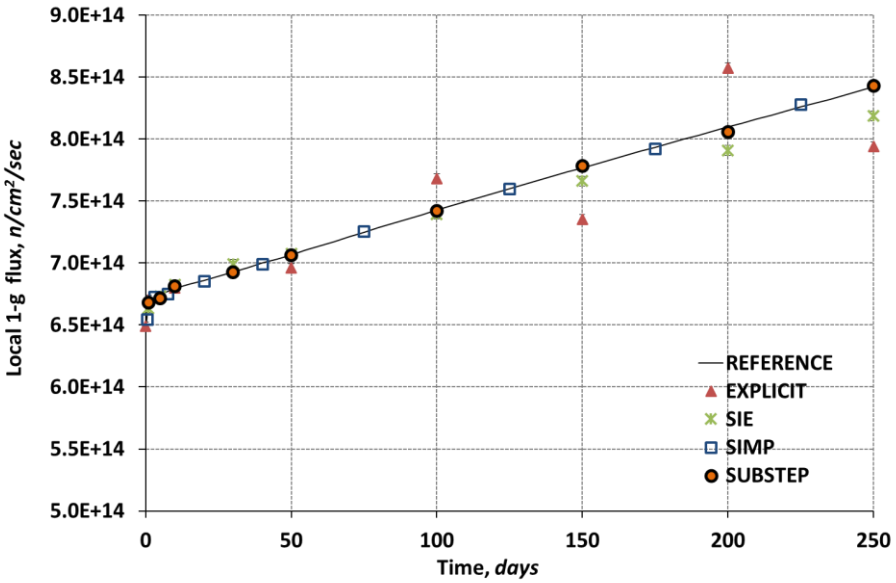

Fig. 11. Comparison of the local (bottom region) flux for various methods, PWR 3D unit cell case

4.3 Thorium Seed-Blanket 3D assembly

The possibility of achieving self-sustainable Th-^{233}U fuel cycle with respect to fissile material was investigated in previous reports and proven to be possible in principle. See for example Volaski et al., (2009), Shwageraus et al., (2009). Fig. 12 shows a schematic view of the seed-blanket design proposed by Kotlyar and Shwageraus (2012). The design parameters are presented in Table 2. Axially, the 366 cm simulated model was divided into 16 active zones and 2 bottom and upper reflector zones. In addition, a non-uniform but fixed coolant density (Kotlyar and Shwageraus, 2013) was used here to invoke the numerical instabilities when the explicit coupling scheme was used. This instability problem was encountered in early analyses of seed-blanket configurations and therefore represents another interesting test case.

Radially, this heterogeneous two fuel zone configuration consists of the seed region containing most of the fissile ^{233}U and a fertile ^{232}Th blanket region. The main idea behind the seed-blanket configuration is to maximize the neutron leakage from the seed zone to the blanket zone and thus achieving maximum neutron capture rate in Th by avoiding competition for neutron absorption with ^{233}U.

The major design challenge associated with SB concept is the high power peaking in the seed zone, which contains high concentration of fissile material. In order to verify thermal hydraulic feasibility of the design, the calculations should be extended to 3D fuel assembly model with TH feedback. The coupled TH analysis are required to assure that all major thermal margin requirements, such as peak fuel central line temperature and minimum departure from nucleate boiling ratio are met. It was found that explicit methods are not reliable for this kind of analyses since they may suffer from numerical (unphysical) instability in distribution of local parameters.

Although SIE methods are stable, the current study suggests that the results obtained with such methods may still significantly deviate from the real solution. This is especially pronounced for the local parameters (e.g. local power) rather than integral parameters (e.g. k-eff).

Here, as in all previous sections, the various coupling schemes were compared to the reference solution. The later was obtained by using the SIE method with ultra-fine timesteps of 2.5 days or 0.04 MWd/kg. It is important to mention that all methods

used the same fine time-steps until 50 days and therefore yield practically identical results up to this time point.

In this study, 200 active fission source iteration cycles with 150,000 histories per cycle were used in neutron transport calculations with MCNP.

Table 2: Design parameters for the seed blanket assembly

Parameter	**Value**
Pin pitch, cm	1.2600
Cladding material	Zircaloy
Blanket fuel pellet radius, cm	0.5300
Blanket cladding outer radius, cm	0.5955
Blanket fuel material	ThH_2-$^{233}UH_3$
Seed fuel pellet radius, cm	0.4095
Seed cladding outer radius, cm	0.4750
Seed fuel material	ThO_2-$^{233}UO_2$
Fuel-cladding thickness, cm	0.0655
Number of pins per assembly	289
Fuel / clad and coolant temperature, K	900/600
Power, W/cm^3	70

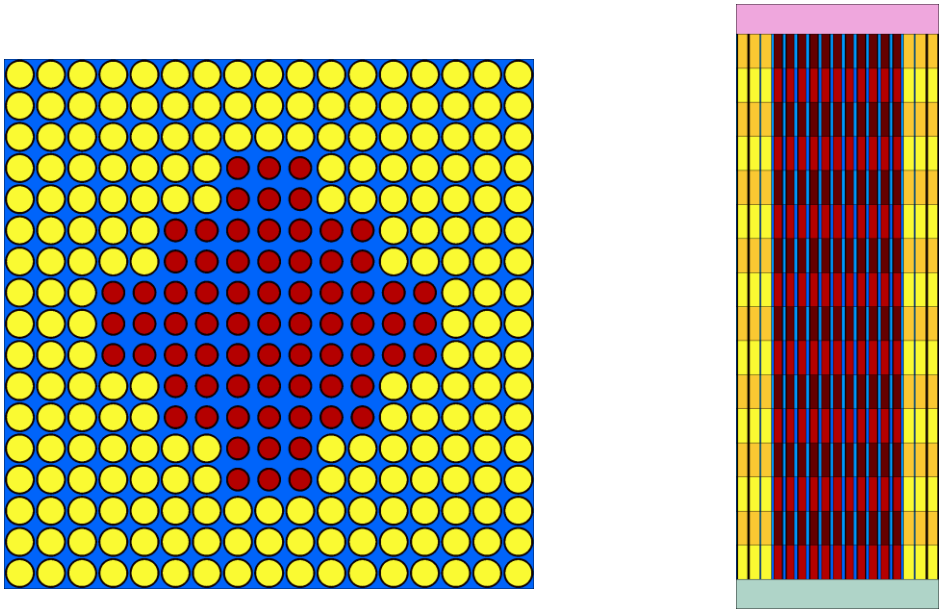

(a) x-y view (b) x-z view

Fig. 12. Thorium seed-blanket 3D fuel assembly

Fig. 13 through Fig. 16 demonstrate the performance of different coupling schemes against the reference solution. One of the main conclusions that can be drawn from these results is that SIE is sensitive to the timestep length. SIMP and SUBSTEP

methods, on the other hand, are much less sensitive and allows for better prediction of criticality (Fig. 13) and concentration of different nuclides, as shown in Fig. 14 through Fig. 16. Finally, Fig. 17, which is of major importance, shows the axial power distribution in the seed for two adjacent depletion steps. Firstly, close examination will reveal that explicit method indeed suffers from numerical instabilities. Secondly, the SIE method, although stable, still notably mis-predicts the power distribution. Finally, SIMP and SUBSTEP very accurately follows the reference power distribution.

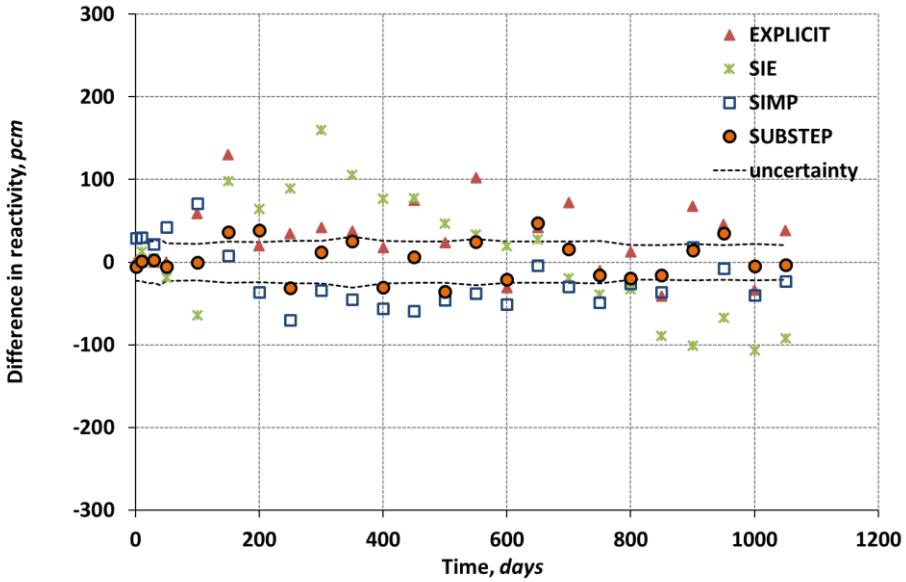

Fig. 13. Comparison of k-inf for various methods, seed-blanket case

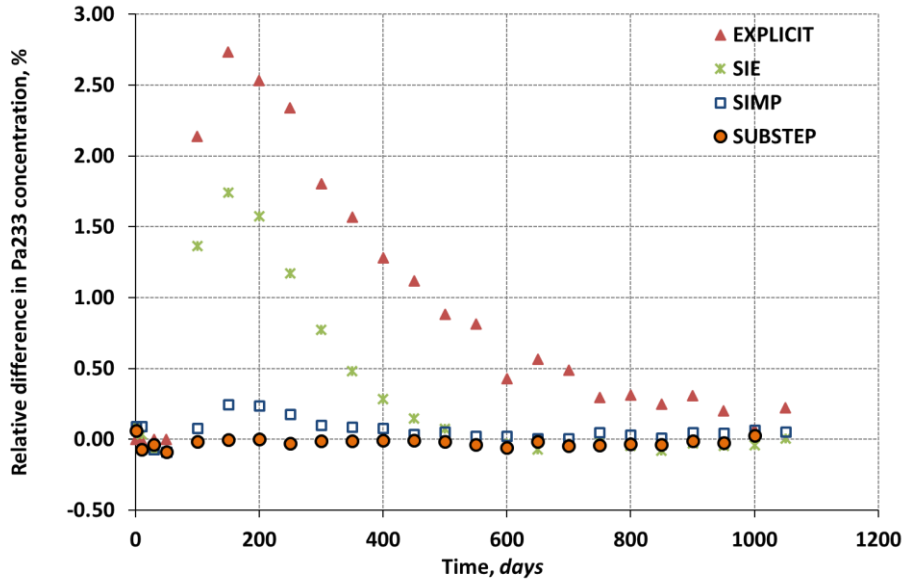

Fig. 14. Relative difference (%) in Pa^{233} concentration, seed-blanket case

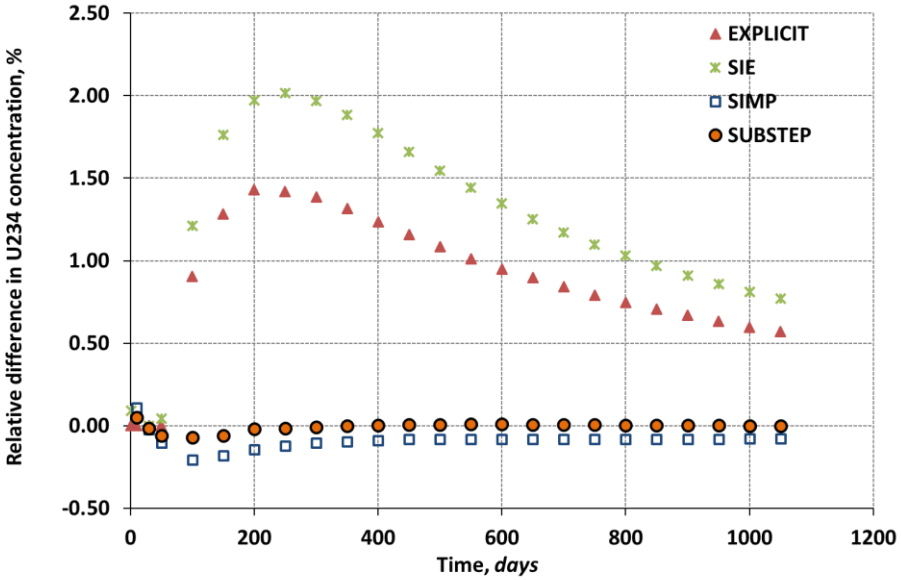

Fig. 15. Relative difference (%) in U^{234} concentration, seed-blanket case

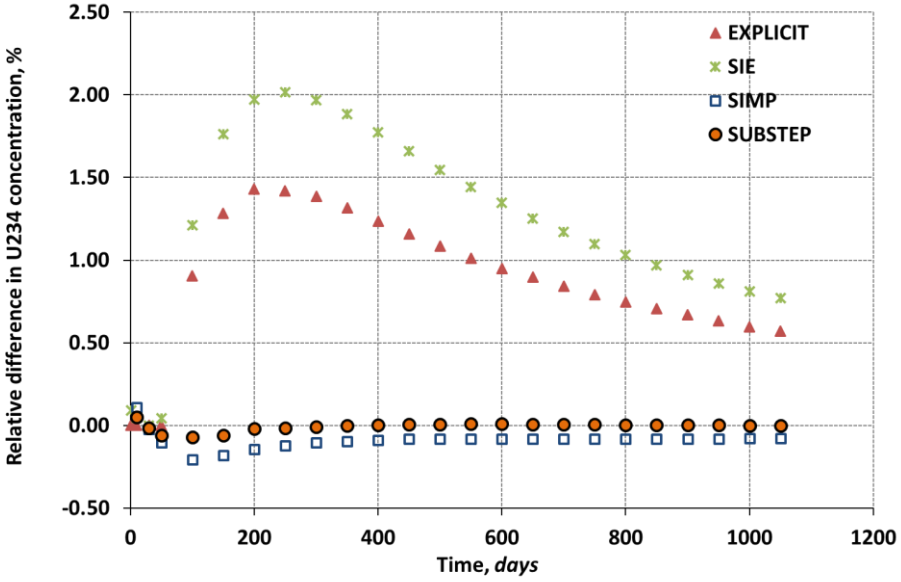

Fig. 16. Relative difference (%) in U^{233} concentration, seed-blanket case

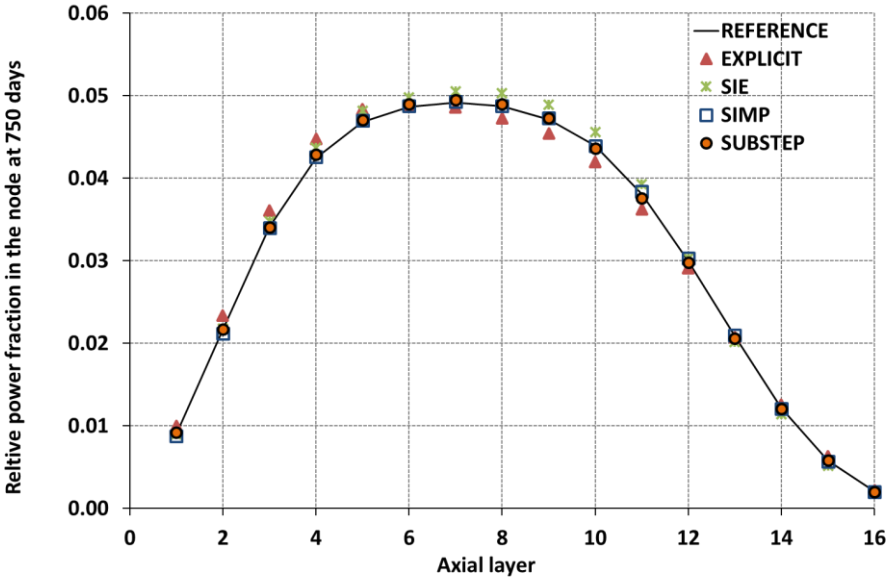

(a) at 750 days

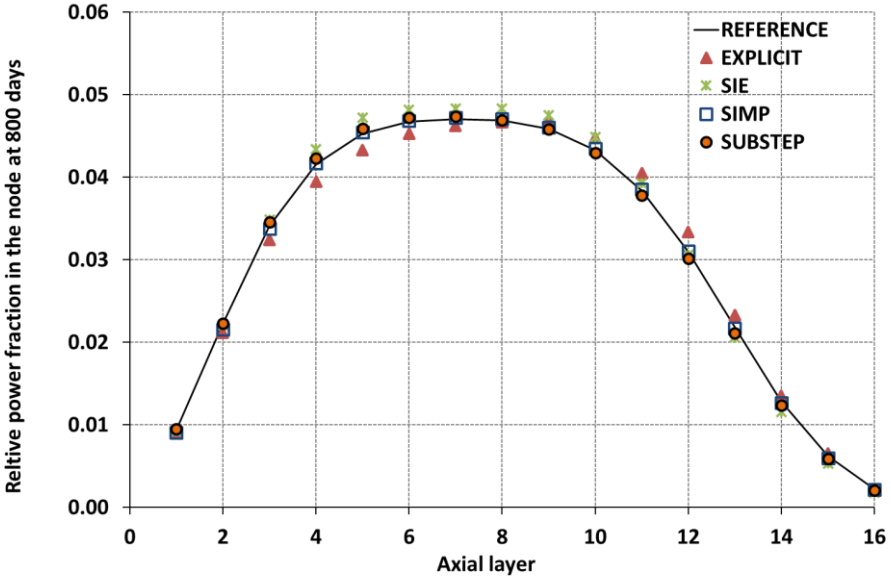

(b) at 800 days

Fig. 17. Power distribution in the seed region, seed-blanket case

5. Summary and Conclusions

Previously, we have investigated the influence of various coupling schemes on the stability of coupled MC calculations. The performance of various explicit approaches was studied. It was shown that these methods can be numerically unstable.

In order to address the numerical stability problem, two alternative coupling approaches were proposed (i.e. SIE and SIMP). In both methods, the depletion and transport problems are solved iteratively. These coupling methods were shown to produce stable results.

However, these methods have not been cross-compared in terms of accuracy. This was one of the main goals of the current study. The analyses carried out here indicate that SIE may produce highly inaccurate results, whereas the solution obtained with SIMP is considerably better but may be improved even further.

In addition, a specific problem associated with the SIE method was reported. SIE is an iterative method that uses the EOS reaction rates to obtain the EOS nuclide densities. In general, this assumption is valid when the depletion steps are truly small and indeed any spectrum variations are negligible. However, when practical timesteps are used the SIE is failing to produce accurate results. Moreover, increasing the number of iterations leads to convergence to even less accurate results, which is unphysical and contradictory to expectations.

Addressing this issue was the primary motivation of this paper. Therefore, the original SIE method was modified to include the substep method. This approach allows accounting for the reaction rates variation within the depletion timestep without the need for additional MC transport solutions. The substep method was combined with an assumption of log-linear correlation between reaction rates and nuclide densities.

Verification of the proposed method was performed on three different 2D and 3D problems. The reference solution was obtained with ultra-fine timesteps. In all the examined cases, the SUBSTEP method demonstrated better performance in terms of accuracy and hence computational efficiency.

The future plans include extending this methodology to incorporate simultaneous burnup-TH substep methodology. In addition, higher order relation between the reaction rates and nuclide density fields can be established to improve the accuracy and the efficiency of this method even further.

References

Bateman H., 1932. Partial Differential Equations of Mathematical Physics. Cambridge, University Press; New York, The Macmillan Co., 522+xii pp.

Bomboni E., Cerullo N., Fridman E., Lomonaco G., Shwageraus E., 2010. Comparison among MCNP-based depletion codes applied to burnup calculations of pebble-bed HTR lattices, Nuclear Engineering and Design, 240 (4), 918-924.

Briesmeister J. F. Ed., 2000. MCNP - A General Monte Carlo N-Particle Code, Version 4C, Los Alamos National Laboratory, LA-13709-M.

Damian F., Brun E., 2015. ORPHEE research reactor: 3D core depletion calculation using Monte-Carlo code TRIPOLI-4®, Annals of Nuclear Energy 82, 203-216.

Dufek J., Gudowski W., 2006. Stochastic Approximation for Monte Carlo Calculation of Steady-State Conditions in Thermal Reactors, Nuclear Science and Engineering, 152, 274-283.

David C. Carpenter and Joseph H. Wolf III, 2010. The Log Linear Rate Constant Power Depletion Method, PHYSOR, Pittsburgh, Pennsylvania, USA, May 9-14.

Dufek J., Hoogenboom J.E., 2009. Numerical Stability of Existing Monte Carlo Burnup Codes in Cycle Calculations of Critical Reactors, Nuclear Science and Engineering, 162, 307-311.

Dufek J., Kotlyar D., Shwageraus E., Leppänen, J., 2013a. Numerical Stability of the Predictor-Corrector Method in Monte Carlo Burnup Calculations of Critical Reactors, Annals of Nuclear Energy, 56, 34-38.

Dufek J., Kotlyar D., Shwageraus E., 2013b. The Stochastic Implicit Euler Method - A Stable Coupling Scheme for Monte Carlo Burnup Calculations, Annals of Nuclear Energy, 60, 295-300.

Dumonteil E., Courau T., 2010. Dominance Ratio Assessment and Monte Carlo Criticality Simulations: Dealing with High Dominance Ratio Systems, Nuclear Technology, 172, 120-131.

Fensin M.L., Hendricks J.S., Trellue H.R., Anhaie S., 2006. The Enhancements and Testing for the MCNPX 2.6.0 Depletion Capability, Journal of Nuclear Technology, 170, 68-79.

Fridman E., Shwageraus E., Galperin A., 2008. Efficient generation of one-group cross sections for coupled Monte Carlo depletion calculations, Nuclear Science and Engineering, 159, 37-47.

Haeck W., Verboomen B., 2007. An optimum approach to Monte Carlo burnup, Nuclear Science and Engineering, 156, 180-196.

Isotalo A. and Aarnio P. A., 2011a. Higher order methods for burnup calculations with Bateman solutions, Annals of Nuclear Energy, 38, 1987-1995.

Isotalo A. and Aarnio P. A., 2011b. Substep methods for burnup calculations with Bateman solutions, Annals of Nuclear Energy, 38, 2509-2514.

Kotlyar D., Shaposhnik Y., Fridman E., Shwageraus E., 2011. Coupled neutronic thermo-hydarulic analysis of full PWR core with Monte-Carlo based BGCore system, Nuclear Engineering and Design, 241 (9), 3777-3786.

Kotlyar D., Shwageraus E., 2012. Neutronic Optimization in High Conversion Th-^{233}U Fuel Assembly with Simulated Annealing, PHYSOR, Knoxville, TN USA, April 15-20.

Kotlyar D., Shwageraus E., 2013. On the use of Predictor-Corrector Method for Coupled Monte Carlo Burnup Codes, Annals of Nuclear Energy, 58, 228-237.

Kotlyar D., Shwageraus E., 2014. Numerically stable Monte Carlo-Burnup-Thermal Hydraulic Coupling Schemes, Annals of Nuclear Energy, 63, 371-381

Leppänen, J., Pusa, M., Viitanen, T., Valtavirta, V. and Kaltiaisenaho, T., 2015. The Serpent Monte Carlo code: Status, development and applications in 2013. Annals of Nuclear Energy, 82, 142-150.

Robbins H. and Monro S., 1951. A Stochastic Approximation Method. Annals of Mathematical Statistics, 22, 400.

Shwageraus E., Volaski D., Fridman E., 2009. Investigation of Fuel Assembly Design Options for High Conversion Thorium Fuel Cycle in PWRs, ANFM 2009, South Carolina.

Sutton T. M., et al., 2007. The MC21 Monte Carlo Transport Code, Joint International Topical Meeting on Mathematics & Computation and Supercomputing in Nuclear Applications, M&C+SNA.

Volaski D., Fridman E., Shwageraus E., 2009. Thermal Design Feasibility of Th-233U PWR Breeder, Global 2009, Paris, France.

Yamamoto A., Tatsumi M. and Sugimura N., 2008. Projected Predictor-corrector Method for Burnup Calculations of Gd-Bearing fuel Assemblies, PHYSOR, Casino-Kursaal Conference Center, Interlaken, Switzerland, September 14-19.